

What and When to Look?: Temporal Span Proposal Network for Video Visual Relation Detection

Sangmin Woo[✉], *Student Member, IEEE*, Junhyug Noh[✉], *Member, IEEE*, and Kangil Kim[✉], *Member, IEEE*

Abstract—Identifying relations between objects is central to understanding the scene. While several works have been proposed for relation modeling in the image domain, there have been many constraints in the video domain due to challenging dynamics of spatio-temporal interactions (*e.g.*, Between which objects are there an interaction? When do relations occur and end?). To date, two representative methods have been proposed to tackle Video Visual Relation Detection (VidVRD): segment-based and window-based. We first point out the limitations these two methods have and propose Temporal Span Proposal Network (TSPN), a novel method with two advantages in terms of efficiency and effectiveness. 1) TSPN tells *what to look*: it sparsifies relation search space by scoring relationness (*i.e.*, confidence score for the existence of a relation between pair of objects) of object pair. 2) TSPN tells *when to look*: it leverages the full video context to simultaneously predict the temporal span and categories of the entire relations. TSPN demonstrates its effectiveness by achieving new state-of-the-art by a significant margin on two VidVRD benchmarks (ImageNet-VidVDR and VidOR) while also showing lower time complexity than existing methods – in particular, twice as efficient as a popular segment-based approach.

Index Terms—Video Visual Relationship Detection (VidVRD), Spatio-temporal Video Understanding, Temporal Span Proposal Network (TSPN).

I. INTRODUCTION

CAPTURING the semantics of the visual scene has long been a concern in computer vision. Despite the remarkable progress of computer vision, understanding visual scenes remains a challenging task. On the way to leap forward, visual relations serve as the stepping stone for narrowing the gap between perceptive and cognitive tasks. A number of works leverages the visual relations including the tasks of image retrieval [1], dynamics prediction [2, 3], image captioning [4, 5], visual question answering [6], image generation [7, 8] and video understanding [9]. The Visual Relation Detection (VRD) task requires modeling both visible information about what

This work was supported by the National Research Foundation of Korea (NRF) grant funded by the Korea government (MSIT) (2019R1A2C109107712), and the Institute of Information & communications Technology Planning & Evaluation (IITP) grant funded by the Korea government (MSIT) (No. 2019-0-01842, Artificial Intelligence Graduate School Program (GIST)). (*Corresponding author: Kangil Kim*)

Sangmin Woo is with the School of Electrical Engineering and Computer Science, Gwangju Institute of Science and Technology, Gwangju 61005, Korea (email: shmwoo9395@gmail.com)

Junhyug Noh is with the Computational Engineering Division, Lawrence Livermore National Laboratory, CA 94550, United States (email: noh1@llnl.gov)

Kangil Kim is with the School of Electrical Engineering and Computer Science and the AI Graduate School, Gwangju Institute of Science and Technology, Gwangju 61005, Korea (email: kangil.kim.01@gmail.com).

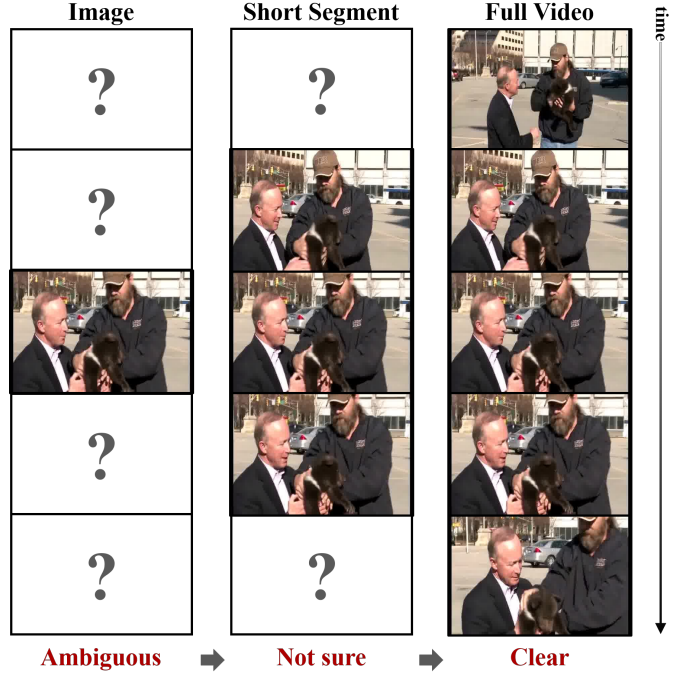


Fig. 1: **Who is handing over the bear to whom?** The relation within a image is equivocal. While guessing relations in short-term video segments is still questionable, the answer becomes clear in full video thanks to the temporal contexts.

and where entities are and underlying information of what interactions are happening between objects in the scene. Relation reasoning is essential in a high-level understanding of the scene. Since a pioneer work of VRD [10] was proposed, several interesting relational reasoning approaches have been studied on the image domain [11, 12, 13]. Recently, a Video Visual Relation Detection (VidVRD) task has been proposed, but due to the difficulty of spatio-temporal relationship modeling, it has not yet been received much attention, and just a handful of works [14, 15, 16, 17, 18, 19, 20] have been proposed.

What makes detecting relations in video difficult? At first glance, we consider the common difficulties of the task. In the view of the object, new objects may appear or disappear due to viewpoint variation or occlusion over time and may also contain motion blur. Therefore, we need to adopt proper object detection [21] and tracking [22, 23] methods. In the view of the relation, it requires modeling long-term temporal dependency and complex dynamics. Relational reasoning in

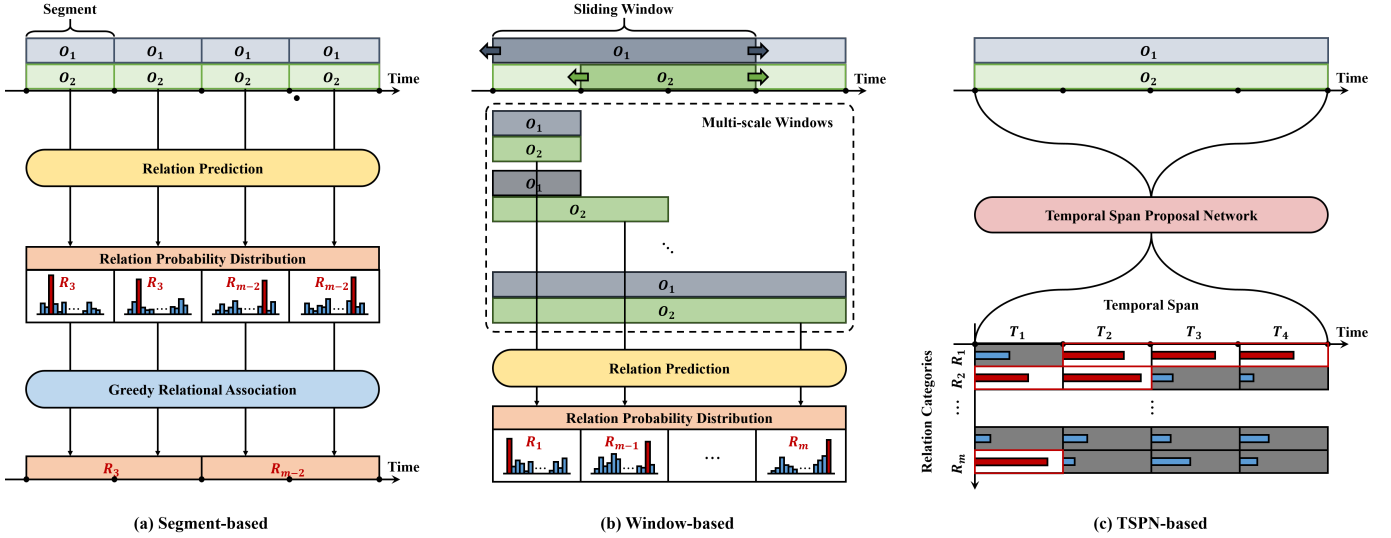


Fig. 2: **Conceptual Comparison of three VidVRD approaches** (empirical comparisons are in Table II, III, VII). (a) **Segment-based approach**: first chunk video into several segments, predict the short-term relations, and then greedily associate the relations of adjacent segments into the long-term relations. (b) **Window-based approach**: first sample a set of sub-tracklet pairs via a size-varying sliding window, and then predict all relations with different temporal span, and (c) **TSPN-based approach (Ours)**: jointly predict relation categories and its temporal span with a single video-level object trajectory pair. O_i stands for i -th object trajectory of all object trajectories in the video, and R_j denotes j -th relation category. We assume that the relations are predicted only for temporal span in which two object trajectories appear simultaneously in the video. Also note that illustration of each method may not contain all the detailed procedures.

the video requires contextual information over time, unlike static images. For example, in Fig. 1, the relation between two men and bear is ambiguous and hard to define with a static image but can be inferred from temporal contexts. Suppose there are n object and m relation categories, the number of possible combinations is $O(n^2 \times m)$. A naive approach to this problem is to learn a distribution over the $n \times n \times m$ lattice space – the complete combinations of objects and relations. However, due to the sparsity of existing relation types and data limits, the model is highly prone to bias. A simple sidestep is to learn low-rank matrices, factorized by object and relations. To put it more simply, the strategy is to separate pipelines of predicting objects and relations, reducing the complexity to $O(n + m)$. To this end, we first detect objects and then predict relations conditionally. Here we further factorize the relation prediction process into two subprocesses: relationness scoring and temporal span proposal. We detail the steps in Sec. III.

To investigate the more complicated issues of the task, we compare existing VidVRD approaches in Fig. 2. They are divided into two approaches: (a) segment-based and (b) window-based. Segment-based approaches [14, 15, 16, 17, 18, 19] first split a video into several segments – typically a segment contains 30 frames, and then predict relations at the segment-level. If the neighboring segments share the same relation triplets, they are merged into a single relation with an extended range. This approach predicts segment-wise relations with only corresponding 30 frames, assuming that the basic relations can always be found in a short duration and can indirectly build the video-level predictions via the association method. However, we argue that 30 frames are not enough to model long-term interactions such as ‘dog–past–person’. Because the relation ‘past’ can only be inferred based on the overall

process by which a dog is behind a person and overtakes a person, continuous monitoring of interactions between objects is required during successive events. More recently, in order to leverage the temporal globality, a window-based approach [20] has been proposed. It adopts a sliding window scheme over the whole object trajectories and obtains all possible sizes of object tracklets. With the object tracklets of various lengths, it can predict both short-term and long-term interactions. However, we see that this is hardly scalable for extremely long videos such as movies because it requires an exhaustive search to sample all combinations of size-varying tracklet pairs to cover various durations of relations, resulting in a cubic complexity.

This work aims to bridge the gap between segment- and window-based methods while improving the shortcomings and exploiting the advantages of the methods with Temporal Span Proposal Network (TSPN) (see Fig. 2(c)). Given a pair of object trajectories, TSPN first finds what pairs of objects are probable to have relations in-between¹, then predicts when the pair-wise relations begin and end. We call the first step *relationness scoring* and the second step *temporal span proposal*. Since it is possible that the object pairs can have multiple relations, we formalize the second step of TSPN as a multi-label classification in practice. By leveraging both temporal locality as in the segment-based approach and temporal globality as in the window-based approach, TSPN can effectively predict pair-wise object relationships. It is also clear that TSPN is more efficient than both methods because it only uses each object pair once to predict all relationships across the video. In particular, it prevents duplicate use of each object tracklet by dividing it into different window lengths, such as the window-based

¹In this paper, we use the term ‘relationness’ to indicate the probability that a relation exists between a pair of objects.

method. By design, the proposed TSPN can coarsen relation search space by capturing the regularity of pair-wise object interaction. Also, TSPN leverages the global video context features, making it strong in both the short and long-term relationship modeling.

We validate TSPN against existing approaches on two popular video visual relation datasets: ImageNet-VidVRD [14] and VidOR [24]. We observe that our method achieved new state-of-the-art on both benchmarks with a significant performance gain. Also, we examine the theoretical computation complexity of three methods (segment, window, and TSPN) and see that TSPN is approximately twice more efficient than the segment-based method. Comprehensive quantitative and qualitative analyses demonstrate the efficacy of TSPN.

II. RELATED WORK

A. Object/Relation Proposals

The Region Proposal Network (RPN) [21] used for the object detection strongly inspired our TSPN. RPN simultaneously predicts object bounds and ‘objectness’ score (we named the term ‘relationness’ after this) to detect the region of interest. In line with RPN, we extend the proposal concept from the space domain to the time domain.

Several recently proposed works also share a similar spirit with TSPN that of reducing search space [20, 25, 26]. However, those approaches are limited to proposing relationships between objects and do not address the time domain.

B. Relation Detection

In an effort to detect relations, numerous studies have been explicitly modeled and adopted neural networks. The challenging and open-ended nature of the task lends itself to various forms. It includes VRD [10, 12] which is the generic form of visual relational reasoning tasks, Human-Object Interaction (HOI) [27, 28, 29] which mainly focuses on human and considers them as the subject, and Scene Graph Generation (SGG) [26, 30, 31, 32, 33, 34] which is a structured form of VRD. Most of the works are mainly conducted in the static image domain.

As a breakthrough, the pioneer work [14] has introduced the first dataset and the baseline of VRD in the dynamic video domain. Since then, just a few works have been proposed due to the difficulty of spatio-temporal modeling. A majority of existing methods follow the segment-based approach [14, 15, 16, 17, 18, 19] which was firstly introduced in [14]. It first breaks a video into segments, predicts per-segment relations, and finally associates relations in a greedy manner. More recently, [20] proposed a window-based approach to handle long-term relations. However, the above-mentioned methods either lack temporal globality or scale poorly for extremely long videos such as movies.

To move one step forward, we introduce a novel TSPN to directly predict relations in an end-to-end manner without the need for many heuristics such as segment length and window size.

III. TEMPORAL SPAN PROPOSAL NETWORK (TSPN)

In this section, we present our novel model Temporal Span Proposal Network (TSPN) for VidVRD. TSPN is constructed on top of the object trajectory proposal module and shares the video-level convolutional features, enabling TSPN to make cost-efficient proposals. An overview of TSPN is shown in Fig. 3, and Table I summarizes the notation about it.

Step	Notation	Description
Object Trajectory Proposal	\mathcal{V}	input video
	f	number of frames in input video
	\mathcal{O}	object trajectories
	n	number of object trajectories
Object-level Feature Extraction	V	visual features
	A_s, A_o, A_u	RoI-Aligned features
	B_s, B_o, B_u	bounding box coordinates
	C_s, C_o, C_u	classification probability distributions
Relationness Scoring	J_s, J_o, J_u	joint features
	\mathcal{S}	relationness scores
	p	number of pair of interests
Relation & Temporal Span Prediction	\mathcal{R}	relation categories
	m	number of relation categories
	\mathcal{T}	temporal spans
	k	number of temporal sectors
	l	coverage per sector
	Z	outer product of \mathcal{R} and \mathcal{T}

TABLE I: **Summary of notations.**

A. Problem Formulation

We design a video relation detector with the notion of object trajectories, relationness, temporal span, and relation labels. Formally, let \mathcal{V} denote an input video, \mathcal{O} be a set of object trajectories and \mathcal{S} , \mathcal{T} and \mathcal{R} denote the relationness score, temporal span, and relation, respectively. The goal is to build a model for $P(\theta_{\text{VidVRD}} = (\mathcal{O}, \mathcal{S}, \mathcal{T}, \mathcal{R}) | \mathcal{V})$. The VidVRD can be factorized into three processes:

$$P(\theta_{\text{VidVRD}} | \mathcal{V}) = \underbrace{P(\mathcal{O} | \mathcal{V})}_{\text{Object Trajectory Proposal}} \underbrace{P(\mathcal{S} | \mathcal{O}, \mathcal{V})}_{\text{Relationness Scoring}} \underbrace{P(\mathcal{T}, \mathcal{R} | \mathcal{S}, \mathcal{O}, \mathcal{V})}_{\text{Relation & Temporal Span Prediction}} \quad (1)$$

The most fundamental yet essential part of relation reasoning is the reliable object detection, since relationships are established via interactions between two objects. Thus, we first detect categories and locations of objects appearing within the video. The rest of the processes are modeled by the TSPN. Specifically, TSPN can be break down into 1) relationness scoring and 2) relation & temporal span prediction subprocesses. Given a set of object trajectory pairs, TSPN first calculates the probability that each pair will have a relation (*i.e.*, relationness), and sample pairs of object trajectories with high relationness (*i.e.*, pair-of-interest). TSPN finally predicts when relations start and end (*i.e.*, temporal span) for all relation categories within a pair-of-interest.

B. Object Trajectory Proposal

The purpose of this step is to find trajectories \mathcal{O} for all n objects present in the video \mathcal{V} with f frames. We adopt the off-the-shelf object detector [21] and tracker [23] to obtain the

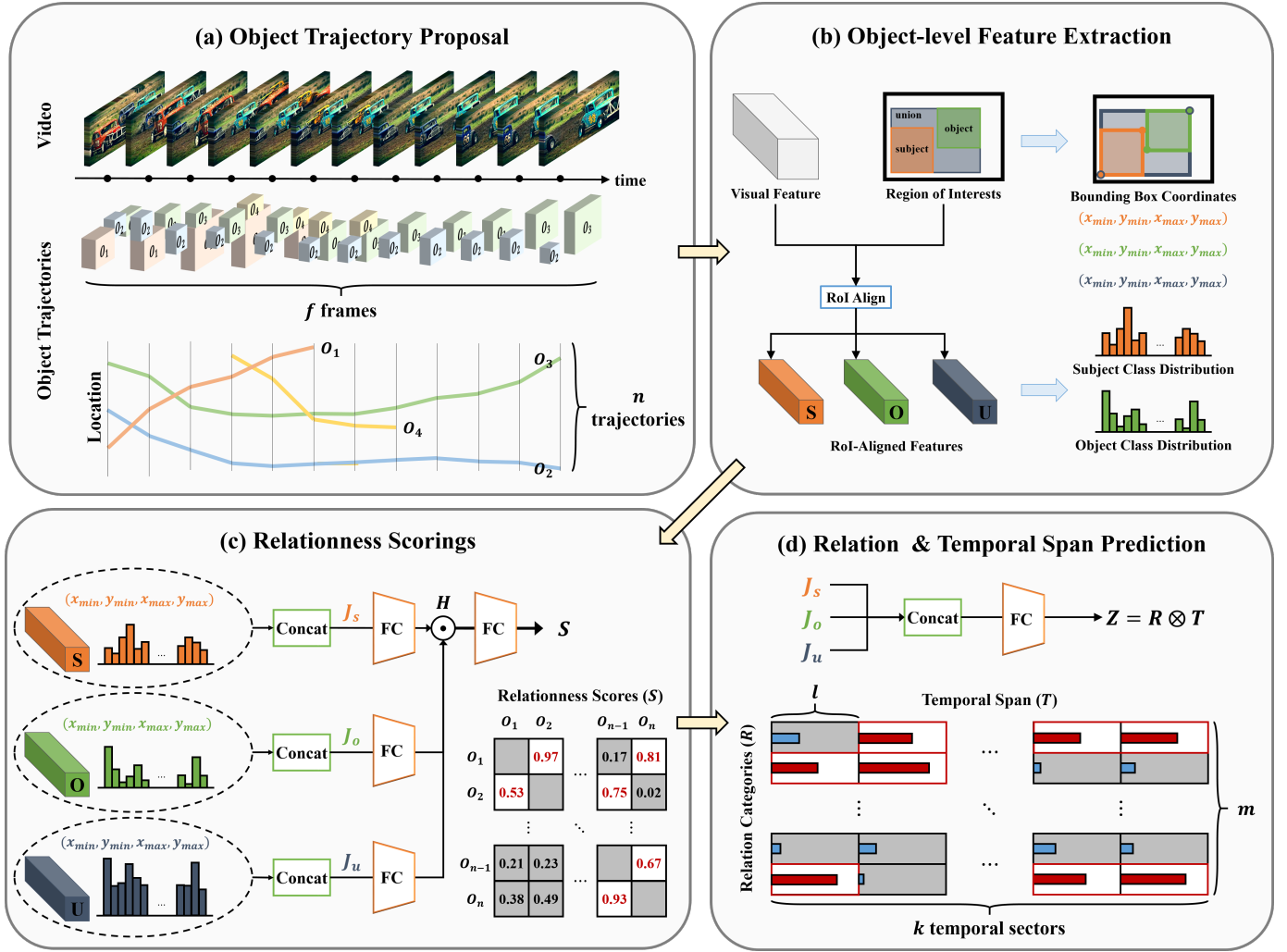


Fig. 3: **Overview of TSPN.** TSPN is built upon the object trajectory proposal head. (a) We first extract video visual features via a pre-trained CNN backbone. (b) With visual features and RoIs, we then obtain RoI-Aligned subject, object, and union features. (c) The features are concatenated with corresponding bounding box coordinates and class distribution, then linearly transformed and fused via a Hadamard product (denoted as \odot in the figure), resulting in a H . The relationness between an object pair is first calculated by feeding H into a Fully-Connected (FC) layer. After then, a set of pairs with high relationness scores (colored in red in the figure) is only considered in the subsequent process. (d) Finally, joint features are concatenated and fed into another FC layer to predict relation labels along with temporal spans.

object trajectory proposals. As all the subsequent processes heavily rely on the object trajectory proposals, it is essential to assure high-quality object trajectories. Thus, we pre-trained object detector. Since the object trajectories have variations in scale, aspect ratio, position, and temporal span, we use Region-of-Interest (RoI) Align [35] to generate fixed 1D representations, easing the subsequent relation computations.

C. Object-level Feature Extraction

Given a video \mathcal{V} , we first extract a set of visual features V via a pre-trained CNN backbone [36]. With V and a pair of object trajectories $(\mathcal{O}_s, \mathcal{O}_o)$ – subscript s and o indicate the semantic identity (subject or object) of object trajectories – we obtain a set of RoI-Aligned features A_s, A_o, A_u by applying RoI-Align [35] operation, where s, o, u denote subject, object, and union RoIs of two object trajectories, respectively. Here, union RoI is a rectangular bound that tightly encompasses the subject RoI and object RoI (see Fig. 3 for better understanding). The

pre-trained object detection head allows us to obtain bounding box coordinates B_s, B_o, B_u . The bounding box coordinates are defined by two points on the lower left and upper right, *i.e.*, $(x_{min}, y_{min}, x_{max}, y_{max})$. Finally, object class distribution C_s, C_o, C_u can be predicted using RoI-Aligned features, where C_u is defined as the sum of C_s and C_o .

D. Relationness Scoring

The computational cost to learn relation distributions for every pair of objects is prohibitively expensive. Only a handful of objects have meaningful relations due to the sparse nature of real-world interactions. In order to model such regularities, we start by scoring relationness between object trajectory proposals. More formally, from n object trajectory proposals \mathcal{O} , the possible pairs are in (n^2) . Our goal here is to sample $p \ll n^2$ pairs.

To this end, we filter out less correlated pairs based on the relationness score. We first jointly model visual, geometric and

semantic relationness by concatenating RoI-Aligned appearance features A_i along with corresponding bounding box coordinates B_i and classification probability distributions C_i , resulting in joint features J_i .

$$J_i = A_i \parallel B_i \parallel C_i, \quad \text{where, } i \in \{s, o, u\} \quad (2)$$

where \parallel is a concatenation operation.

Then, relationness scores S is calculated as follows:

$$H = \mathbf{W}_s^T J_s \odot \mathbf{W}_o^T J_o \odot \mathbf{W}_u^T J_u + \mathbf{B}_h \quad (3)$$

$$S = \sigma(\mathbf{W}_s^T H + \mathbf{B}_s) \quad (4)$$

where \mathbf{W} and \mathbf{B} respectively denotes weight matrix and bias matrix, \odot indicates Hadamard product, and σ is a non-linear activation, which maps any real values into a finite interval (e.g., sigmoid).

After iterating the process over every object trajectory pairs existing in the video, we sort the output relationness scores in descending order and maintain only the top- p pair-of-interests per video. Only these are considered in subsequent processes.

E. Relation & Temporal Span Prediction

Due to the video's dynamic characteristic, numerous relations can exist within multiple time span between a single pair of object trajectories. This means that different relation instances can exist in a different time span as well as in the same time span. For example, think of racehorses. They first stand side by side, move ahead, and compete during the race. Even to simplify the situation, it would be horse1 – stand next to – horse2 in the early timespan, and horse1 – chase – horse2 in the late timespan. Therefore, we need to simultaneously predict what relations exist and the range of time they occur, given the object trajectory pair.

There is an open choice in predicting the temporal span of relations. RPN [21] suggests using anchors in different scales with a sliding window scheme and learn to reduce the localization error for region proposal. However, when it comes to temporal span proposal, it becomes unnecessary since relation detection does not require fine-grained temporal duration to match the ground-truth. We thus are not using the anchor or sliding-window scheme in this work. The brute-force approach to find temporal span is to learn a probability distribution over the $m \times f$ lattice space – the number of relation categories is m , and the total number of frames is f – which is highly costly. To conform with the parsimonious property, we simplify the process by quantizing the video-level temporal span into several sectors; we then predict the likelihood of each relation category's presence within the sectors. This strategy is distinguished from the segment-based approaches in terms of the feature level because it is not possible to encode the video-level temporal contexts by extracting features from segments. In contrast, we use the video-level features and predict relations with just a single glance at a video. In other words, there is no need to chunk into overlapping short segments or repeat computation over the same part. That is, TSPN can directly specify relationship ranges and categories across the whole video without redundancy.

Let the time span over which two object trajectories intersect (*i.e.*, $O_s \cap O_o$) as \mathcal{T} . After \mathcal{T} breaks down into k temporal sectors, one sector is responsible for the range l of the entire time span. In other words, each temporal sector per pair-of-interest covers a length of l , which is calculated as:

$$l = \frac{1}{k} (\text{len}(\mathcal{O}_s \cap \mathcal{O}_o)) \quad (5)$$

where $\text{len}(\cdot)$ stands for the length of a given trajectory.

We can now discretely predict the temporal sectors in which the relations exist instead of predicting the temporal span directly in continuous video space. We concatenate joint features J_s, J_o, J_u and feed into a fully-connected layer followed by a non-linearity.

$$Z = \sigma(\mathbf{W}_z^T (J_s \parallel J_o \parallel J_u) + \mathbf{B}_z) \quad (6)$$

where the output matrix $Z \in \mathbb{R}^{m \times k}$ represents the outer product (denoted as \otimes the equation below) of the probability distribution of relation categories $\mathcal{R} \in \mathbb{R}^m$ and that of temporal span $\mathcal{T} \in \mathbb{R}^k$, enabling multi-label classification within multiple time spans.

$$Z = \mathcal{R} \otimes \mathcal{T} \quad (7)$$

F. Loss Function

The whole network can be trained in an end-to-end manner. Total loss is sum of relationness (\mathcal{L}_R) and temporal span (\mathcal{L}_T) loss. Both are binary cross entropy loss.

$$\mathcal{L}_{\text{total}} = \mathcal{L}_R + \mathcal{L}_T \quad (8)$$

\mathcal{L}_R measures the loss between p pair of ground truth binary values r^* (pair-of-interest as 1, otherwise 0) and the predicted relationness (r in Eq. (4)).

$$\mathcal{L}_R = -\frac{1}{p} \sum_{i=1}^p r^* \cdot \log r + (1 - r^*) \cdot \log(1 - r) \quad (9)$$

\mathcal{L}_T measures the loss between $m \times k$ pair of ground truth temporal spans t^* and predicted temporal spans t .

$$\mathcal{L}_T = -\frac{1}{m \times k} \sum_i^{m \times k} t^* \cdot \log t + (1 - t^*) \cdot \log(1 - t) \quad (10)$$

We construct a ground truth temporal span into a set of temporal sectors with values of 0 or 1, each of which is set to 1 if the relation lasts more than half within that temporal sector, otherwise set to 0.

IV. EXPERIMENTS

In this section, we conduct comprehensive studies to validate the effectiveness and efficiency of the proposed TSPN. Here, we report results on two challenging dataset: ImageNet-VidVRD [14] and VidOR [24]. To understand the behavior of TSPN, we provide extensive quantitative analyses. Also, we present qualitative results to examine how our model can benefit from temporal globality concretely. Finally, we compare the estimated computation time of TSPN with two representative VidVRD methods (segment-based and window-based).

Approach	Model	VRDet			VRTag		
		R@50	R@100	mAP	P@1	P@5	P@10
Segment	VidVRD [14]	5.54	6.37	8.58	43.00	28.90	20.80
	MHRA [15]	6.82	7.39	13.27	41.00	28.70	20.95
	GSTEGL [16]	7.05	8.67	9.52	51.50	39.50	28.23
	VRD-GCN [17]	8.07	9.33	16.26	57.50	41.00	28.50
	MHA [19]	9.53	10.38	19.03	57.50	41.40	29.45
Window	PPN-STGCN [20]	11.21	13.69	18.38	60.00	43.10	32.24
TSPN (Ours)		11.56	14.13	18.90	60.50	43.80	33.73

TABLE II: Comparison with recent approaches on ImageNet-VidVRD [14] dataset.

Approach	Model	VRDet			VRTag		
		R@50	R@100	mAP	P@1	P@5	P@10
Segment	MMFF [18]	6.89	8.83	6.56	51.20	40.73	-
	MHA [19]	6.35	8.05	6.59	50.72	41.56	32.53
Window	PPN-STGCN [20]	8.21	9.90	6.85	48.92	36.78	-
	TSPN (Ours)	9.33	10.71	7.61	53.14	42.22	34.94

TABLE III: Comparison with recent approaches on VidOR [24] dataset.

A. Implementation Details

We first generate bounding boxes at each frame using Faster R-CNN [21] equipped with ResNet-101 [36] backbone. The detector is trained on train/val images of 35 object categories – which are used in the ImageNet-VidVRD [14] dataset – of MS-COCO [37] and ILSVRC2016-DET [38] datasets. To be consistent with [20], we perform Non-Maximum Suppression (NMS) in the detection phase with IoU threshold = 0.5 to reduce the redundant bounding boxes since NMS in the tracking phase might wrongly remove the overlapping trajectories with different classes since it is class-agnostic. As an object tracker, we adopt deep SORT [23], which integrates visual appearance information to gain robustness against identity switching while associating the objects with the same identity in neighboring frames. We set the number of pair-of-interests as 64 (*i.e.*, $p = 64$). For the Eq. (5), the number of sectors is set to 16 (*i.e.*, $k = 16$). We keep top-100 relation triplet predictions per video.

B. Dataset Configuration

In both datasets, objects and relation triplets (with temporal span) are annotated in the form of $\{\text{trajectory id}, \text{category}, \text{bounding box coordinates}\}$ and $\{(\text{subject id} - \text{predicate category} - \text{object id}), (\text{start frame} - \text{end frame})\}$, respectively. We exclude several unannotated videos in the experiment.

a) ImageNet-VidVRD: ImageNet-VidVRD [14] is a subset of ILSVRC2016-VID [38] train and validation set. Videos are selected with the criteria of whether they contain clear visual relations. It contains 1,000 videos (train:test split is 800 : 200) with the manually labeled object categories, corresponding bounding box trajectories, and relation triplets. It covers 35 and 132 categories for objects and predicates, respectively. Note that the relations in the training set are all annotated in the segment-level (*e.g.*, 30 frames). Thus, we link them into the video-level relations in order to directly optimize long-term relations.

b) VidOR: VidOR [24] is a large-scale video dataset which contains 10,000 videos (train:val:test split is 7,000 : 835 : 2,165) from YFCC100M [39] collection. The average video length in train/val set is ~ 36 seconds, totaling ~ 84 hours. It contains 80 categories of objects with trajectories to indicate their spatio-temporal location in the videos, 50 categories of relation predicates, and carefully annotated the relation triplets. This results in around 50,000 objects and 380,000 relation instances annotated. Only the training and validation set were used for the experiment because the test set is not yet publicly available.

C. Evaluation Protocol

We follow the standard evaluation task settings and metrics [14] listed below:

a) Tasks: In *Visual Relation Detection (VRDet)* task, given a video, the objective is to jointly predict object trajectories, categories, and existing relations with its duration. The object trajectories are considered matched only if vIoU^2 with the ground truth trajectory is greater than half.

In *Visual Relation Tagging (VRTag)* task, given video with a set of ground truth object trajectories, the objective is to find all object categories and existing relations. In other words, it needs to detect the relation triplet $\langle \text{subject} - \text{predicate} - \text{object} \rangle$ correctly.

In both tasks, detected visual relation instances are treated as correct only if the trajectories of subject and object that form the relation both have sufficiently high vIoU (*i.e.*, $\text{vIoU} > 0.5$) with the ground truth.

b) Evaluation metrics: For *Visual Relation Detection (VRDet)* task, we adopt mean Average Precision (*mAP*) and *Recall@K* to evaluate the detection performance. Specifically, we use video-wise *Recall@50* and *Recall@100*, which measures the fraction of the top-*K* predictions among the ground-truth triplets. Following [14], we also report the *mAP* metric

² vIoU denotes the volumetric intersection over the union of two trajectories.

Exp	Ablations		VRDet			VRTag		
	\mathcal{R}	\mathcal{T}	$R@50$	$R@100$	mAP	$P@1$	$P@5$	$P@10$
1			6.14	7.52	9.38	40.50	28.90	21.95
2	✓		9.62	11.69	16.29	57.00	41.90	30.45
3		✓	9.95	12.35	15.93	54.50	40.20	29.50
4	✓	✓	11.56	14.13	18.90	60.50	43.80	33.73

TABLE IV: **Model ablations.** \mathcal{R} and \mathcal{T} denotes relationness scoring and temporal span proposal modules, respectively.

to evaluate the overall precision performance at different recall values.

For *Visual Relation Tagging (VRTag)* task, *Precision@K* as the evaluation metric to emphasize the ability to tag accurate visual relations. It measures the fraction of ground-truth among the top- K triplets. Specifically, we use video-wise *Precision@1*, *Precision@5*, and *Precision@10* since the number of visual relation instances per segment is 9.5.

D. Comparison with State-of-the-Art

We compare TSPN with state-of-the-art approaches on the two VidVRD benchmarks: ImageNet-VidVRD [14] and VidOR [24]. As a comparison, we consider following methods: VidVRD [14], MHRA [15], GSTEG [16], VRD-GCN [17], MMFF [18], MHA [19] and PPN-STGCN [20]. VidVRD detects relations in the short-term and greedily associates them. MHRA generates multiple hypotheses for video relation instances for more robust long-term relation prediction. GSTEG constructs a conditional random field on a spatio-temporal graph exploiting the statistical dependency of relational entities. VRD-GCN passes the message through fully-connected spatial-temporal graphs and conducts reasoning in the 3D graphs using Graph Convolution Network (GCN) [40]. MMFF predicts relations by jointly using spatial-temporal visual feature and language context feature. MHA maintains multiple possible relation hypotheses during the association process to handle the inaccuracy of the former steps. PPN-STGCN employs a sliding-window scheme to predict both short-term and long-term relationships and utilizes GCN to calculate the compatibility of tracklet proposal pair. Existing VidVRD approaches can be divided into two families: segment-based [14, 15, 16, 17, 19] and window-based [20] approaches. Results are presented in Table II and Table III. We observe that TSPN achieves new state-of-the-art results on both VidVRD benchmarks, demonstrating its effectiveness among the competing methods. TSPN leverages the complementariness of multiple information, and is designed to utilize the spatio-temporal contexts of the entire video, making it strong not only for the short-term but also for the long-term relations.

E. Quantitative Analysis

The experiments are conducted on the ImageNet-VidVRD.

a) TSPN Ablations: We consider several ablations on building blocks of TSPN to identify how each component contributes to the performance and verify its efficacy. Ablation results are summarized in Table IV. Without both relationness scoring (\mathcal{R}) and temporal span proposal (\mathcal{T}) (equivalent to Exp 1), we have to optimize $m \times l$ distribution for n^2 pairs,

Exp	No. of PoIs (p)	VRDet			VRTag		
		$R@50$	$R@100$	mAP	$P@1$	$P@5$	$P@10$
1	16	9.85	11.84	18.03	62.00	44.60	34.96
2	32	10.32	12.93	18.41	61.50	44.10	34.04
3	64	11.56	14.13	18.90	60.50	43.80	33.73
4	128	10.92	14.29	18.29	57.50	43.10	32.68

TABLE V: **Optimal number of Pair-of-Interests (PoIs).**

Exp	No. of sectors (k)	VRDet			VRTag		
		$R@50$	$R@100$	mAP	$P@1$	$P@5$	$P@10$
1	4	5.19	6.25	9.79	33.50	23.10	15.44
2	8	10.02	11.49	14.74	49.00	36.50	24.04
3	16	11.56	14.13	18.90	60.50	43.80	33.73
4	32	11.32	14.50	18.69	59.50	42.60	33.14

TABLE VI: **Adequate quantization of temporal span.**

but with both \mathcal{R} and \mathcal{T} (equivalent to Exp 4), we only need to optimize $m \times k$ distribution for p pairs, where $p \ll n^2$ and $k \ll l$. In this experiment, we can see that the \mathcal{R} and \mathcal{T} are complementary to each other in constructing a strong VidVRD model.

b) Optimal Size of Relation Search Space: We further explore the optimal number of pair-of-interest (p) per video. Considering that VidVRD contains 4,835 video-level relation instances in 200 test set (~ 24 instances per video on average), we set the number of pair-of-interest as 32 by default. We examine several variations ($p = 16$ or 64 or 128) in Table V. Although 16 shows the highest precision since it has a low false-positive rate, 64 holds the best overall results. The results indicate that balancing positives and negatives labels is crucial since the TSPN learns from penalizing the false positives. The number of PoIs should be appropriately set because the resulting sampled object pairs affect the subsequent processing. If it is too large (*e.g.*, 128), the probability of the noisy object pairs being included in the PoIs becomes higher and result in degraded performance. We empirically found that 64 works well, and use this number for the rest of the experiments.

c) Trade-off in Temporal Span Quantization: We investigate the effect of quantizing the temporal span proposals into sectors (k in Eq. (5)). Since the length of the videos varies, each video has a different quantization impact. Sparse quantization narrows the search space (*i.e.*, easy to optimize) but lowers the matching rate at the same time. On the other hand, dense quantization increases the matching rate, but it also widens the search space (*i.e.*, expensive to optimize). We conduct an experiment in Table VI to assess the optimal degree of quantization. We can observe the best results when the number of sectors is set to 16.

F. Qualitative Analysis

To better see how TSPN understands the dynamics of spatio-temporal interactions, we provide qualitative examples in Fig. 4. Here, we compare TSPN with VidVRD [14], which first proposed a popular segment-based approach. The results show that the VidVRD often fails to capture long-term relations since it relies on temporally local features. On the other hand, TSPN successfully identifies them. For example,

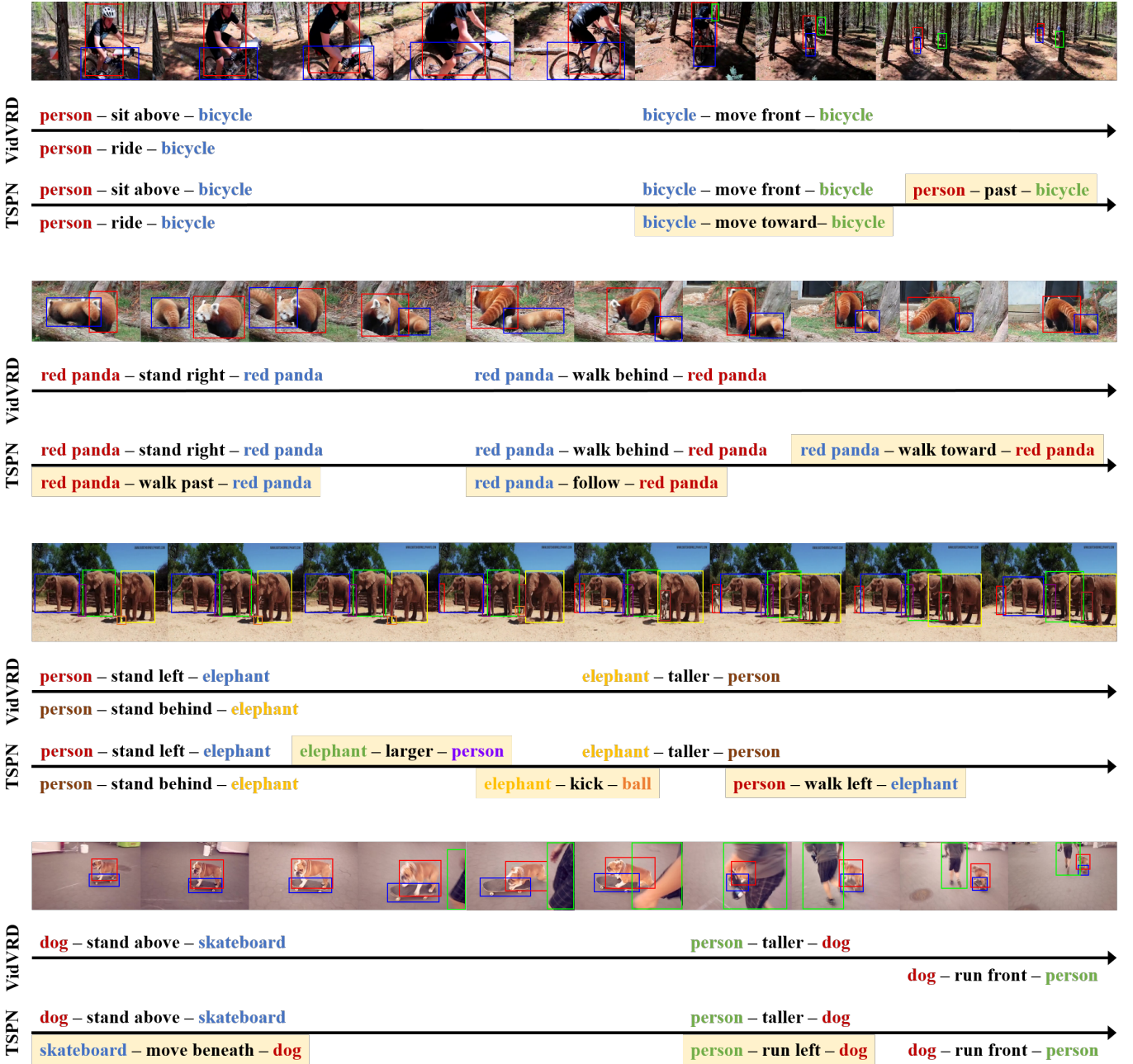


Fig. 4: **Qualitative examples of visual relation detection results.** For comparison, we contrast the predicted relation triplets (*i.e.*, subject-relation-object) of VidVRD with those of TSPN for each given video. The same color means the same object instance. The arrows represents the time axis, providing an approximation of the temporal span of the predicted relation triplets. We highlight relations that TSPN correctly predicted, while VidVRD does not. The predicted relations are considered correct only if the pair of object trajectories have sufficiently high vIoU (*i.e.*, $\text{vIoU} > 0.5$) with ground truth trajectories, and only the correct relations of the top-20 predictions are shown in the figure.

the relation **person-past-bicycle** (105–150)³ can only be detected by understanding the long-term relationship since the model should capture the entire process of person being behind bicycle and catching up with bicycle as it moves forward. It goes the same for the relation **red panda-walk past-red panda** (0–75). TSPN also detects more active or sophisticated relations such as **elephant-kick-ball** (0–60) and **skateboard-move**

beneath-dog (0–360), while VidVRD simply detects trivial relations (*e.g.*, **elephant-taller-person**, **person-taller-dog**), which can also be predicted in a still image. This also reveals the limitation of segment-based methods. That is, it cannot leverage the video-level context. The reason is that VidVRD is unable to directly utilize the temporally global feature since it predicts relations in the segment-level and aggregates them into the video-level relation. In contrast, TSPN can directly predict long-term relations from the proposed temporal span.

³The numbers in parentheses mean ground truth “begin frame – end frame”.

Method	Approximated Time	Upper Bound	Typical Setting ($s = \frac{l}{2}$)	Big- O
Segment-based	$\left\lceil \frac{L-l+s}{s} \right\rceil$	$\frac{L-l+2s}{s}$	$\frac{2L}{l}$	$O(L)$
Window-based	$\sum_{k=1}^{\frac{L}{l}} \left\lceil \frac{L-kl+s}{s} \right\rceil$	$\left(\frac{L^2}{s} - \frac{L^2}{2l^2s} - \frac{L}{2ls} + 2L \right)^2$	$\left(\frac{2L^2}{l} - \frac{L^2}{l^3} - \frac{L}{l^2} + 2L \right)^2$	$O(L^4)$
TSPN-based (ours)	$\frac{L}{l}$	$\frac{L}{l}$	$\frac{L}{l}$	$O(L)$

TABLE VII: **Comparison of estimated computation time with existing approaches.** L denotes the intersection of subject trajectory and object trajectory (*i.e.*, pair-of-interest), l denotes segment length or minimum window size or coverage of each temporal sector, and s denotes the stride of segment or window, where $s < l \ll L$.

G. Comparison of Estimated Computation Time

To observe the efficiency of TSPN, we compare TSPN with two representative VidVRD approaches (segment-based and window-based) in terms of estimated computation time. The segment-based approach predicts relations by dividing the video into several segments and connecting to long relations if adjacent relations are the same. The window-based approach first obtains multiple tracklets by sliding multi-size windows over the trajectories, finds tracklet pairs with high similarity via a correlation embedding module, and finally predicts the relations for the valid pairs. TSPN first finds out what object trajectory pairs are highly likely to have relations by calculating relationness score, then TSPN simultaneously predicts relation categories and their temporal span with sampled pairs.

Note that direct comparisons are difficult as the greedy association in the segment-based approach is an offline algorithm, and the source codes of the window-based approach are not publicly available. We thus provide the asymptotic computational complexity of each method for relation prediction. Here, we do not consider additional features or modules (*e.g.*, greedy association, pair correlation embedding module, and relationness scoring) other than the main components for simplicity. Also, we consider that the segment length of the segment-based approach, a minimum window size of the window-based approach, and coverage per temporal sector in TSPN are all on the same scale. Now the time complexity can be represented by the number of object pairs to consider, assuming that predicting relations for each pair of objects takes the same amount of time.

Let the intersection of subject and object be L , segment or minimum-window or sector length be l , and stride be s . Intuitively, the computation time of segment-based approach is proportional to the number of segments. The number of segments can be calculated as:

$$\mathbb{N}_s = \left\lceil \frac{L-l+s}{s} \right\rceil \quad (11)$$

Similarly, the window-based method depends on the number of windows. The window-based method exhaustively uses window of all sizes, from smallest (*i.e.*, l) to largest (*i.e.*, L), to capture both the short-term and long-term object relations. The number of all windows can be calculated as:

$$\mathbb{N}_w = \sum_{k=1}^{\frac{L}{l}} \left\lceil \frac{L-kl+s}{s} \right\rceil \quad (12)$$

Since relation detection requires two windows each responsible for subject and object, the overall computation shows a quadratic growth rate with respect to the number of windows.

In contrast, TSPN directly predicts the relationship categories and their temporal span using the entire video context only once. Thus, it shows a linear growth rate with respect to the number of temporal sectors. Since there is no overlap between sectors, the number of sectors can be simplified as:

$$\mathbb{N}_t = \frac{L}{l} \quad (13)$$

Under the condition of $s < l$, we can obtain the following conclusions⁴:

$$\mathbb{N}_t < \mathbb{N}_w < \mathbb{N}_s \quad (14)$$

which means that TSPN is always more efficient than the segment and window-based approaches. In practice, we follow the typical settings of stride/segment length ratio ($s = 15$, $l = 30$; thus, $s = l/2$), so the estimated computation time of segment and TSPN-based approaches are proportional to $\frac{L}{s}$ and $\frac{L}{l}$, respectively. Therefore, TSPN is approximately $2 \times$ more efficient than the segment-based approach. The overall estimated computation times are summarized in Table VII.

V. CONCLUSION

This work introduces a novel Temporal Span Proposal Network (TSPN) for Video Visual Relation Detection (VidVRD). TSPN effectively reduces the relational search space by learning which object pairs should be considered based on the relationness score between object trajectory pairs. TSPN simultaneously predicts the temporal span and categories of the entire relations with a single global video feature, which is not only efficient but also effective in predicting both short and long-term relations. We validate the TSPN through comprehensive experiments. TSPN establishes a strong baseline for VidVRD by leveraging the complementarity of the two key modules. In particular, TSPN achieves new state-of-the-art performance on two VidVRD benchmarks (ImageNet-VidVRD and VidOR) without many external algorithms or heuristics (*e.g.*, greedy association, window sliding) commonly seen in previous approaches while theoretically faster than conventional approaches – $2 \times$ faster than segment-based approach.

⁴Here is a simple derivation:

1) \mathbb{N}_w can be rewritten as $\mathbb{N}_s + \sum_{k=2}^{\frac{L}{l}} \left\lceil \frac{L-kl+s}{s} \right\rceil$; therefore, $\mathbb{N}_s < \mathbb{N}_w$.
2) The lower bound of \mathbb{N}_s is $\frac{L-l}{s} + 1$; since $s < l$, it satisfies: $\frac{L-l}{s} + 1 > \frac{L-l}{l} + 1 = \frac{L}{l} = \mathbb{N}_t$; therefore, $\mathbb{N}_t < \frac{L-l}{s} + 1 \leq \mathbb{N}_s$.

REFERENCES

[1] J. Johnson, R. Krishna, M. Stark, L.-J. Li, D. Shamma, M. Bernstein, and L. Fei-Fei, "Image Retrieval Using Scene Graphs," in *CVPR*, 2015, pp. 3668–3678.

[2] A. Santoro, D. Raposo, D. G. Barrett, M. Malinowski, R. Pascanu, P. Battaglia, and T. Lillicrap, "A Simple Neural Network Module for Relational Reasoning," in *NeurIPS*, 2017, pp. 4967–4976.

[3] P. W. Battaglia, R. Pascanu, M. Lai, D. Rezende, and K. Kavukcuoglu, "Interaction Networks for Learning About Objects, Relations and Physics," *arXiv preprint arXiv:1612.00222*, 2016.

[4] T. Yao, Y. Pan, Y. Li, and T. Mei, "Exploring Visual Relationship for Image Captioning," in *ECCV*, 2018, pp. 684–699.

[5] X. Yang, K. Tang, H. Zhang, and J. Cai, "Auto-Encoding Scene Graphs for Image Captioning," in *CVPR*, 2019, pp. 10 685–10 694.

[6] D. Teney, L. Liu, and A. van Den Hengel, "Graph-Structured Representations for Visual Question Answering," in *CVPR*, 2017, pp. 1–9.

[7] J. Johnson, A. Gupta, and L. Fei-Fei, "Image Generation From Scene Graphs," in *CVPR*, 2018, pp. 1219–1228.

[8] O. Ashual and L. Wolf, "Specifying Object Attributes and Relations in Interactive Scene Generation," in *ICCV*, 2019, pp. 4561–4569.

[9] C.-Y. Ma, A. Kadav, I. Melvin, Z. Kira, G. AlRegib, and H. Peter Graf, "Attend and Interact: Higher-Order Object Interactions for Video Understanding," in *CVPR*, 2018, pp. 6790–6800.

[10] C. Lu, R. Krishna, M. Bernstein, and L. Fei-Fei, "Visual Relationship Detection With Language Priors," in *ECCV*. Springer, 2016, pp. 852–869.

[11] B. Dai, Y. Zhang, and D. Lin, "Detecting Visual Relationships With Deep Relational Networks," in *CVPR*, 2017, pp. 3076–3086.

[12] H. Zhang, Z. Kyaw, S.-F. Chang, and T.-S. Chua, "Visual Translation Embedding Network for Visual Relation Detection," in *CVPR*, 2017, pp. 5532–5540.

[13] S. Jae Hwang, S. N. Ravi, Z. Tao, H. J. Kim, M. D. Collins, and V. Singh, "Tensorize, Factorize and Regularize: Robust Visual Relationship Learning," in *CVPR*, 2018, pp. 1014–1023.

[14] X. Shang, T. Ren, J. Guo, H. Zhang, and T.-S. Chua, "Video Visual Relation Detection," in *ACMMM*, 2017, pp. 1300–1308.

[15] D. Di, X. Shang, W. Zhang, X. Yang, and T.-S. Chua, "Multiple Hypothesis Video Relation Detection," in *BigMM*. IEEE, 2019, pp. 287–291.

[16] Y.-H. H. Tsai, S. Divvala, L.-P. Morency, R. Salakhutdinov, and A. Farhadi, "Video Relationship Reasoning Using Gated Spatio-Temporal Energy Graph," in *CVPR*, 2019, pp. 10 424–10 433.

[17] X. Qian, Y. Zhuang, Y. Li, S. Xiao, S. Pu, and J. Xiao, "Video Relation Detection With Spatio-Temporal Graph," in *ACMMM*, 2019, pp. 84–93.

[18] X. Sun, T. Ren, Y. Zi, and G. Wu, "Video Visual Relation Detection via Multi-Modal Feature Fusion," in *ACMMM*, 2019, pp. 2657–2661.

[19] Z. Su, X. Shang, J. Chen, Y.-G. Jiang, Z. Qiu, and T.-S. Chua, "Video Relation Detection via Multiple Hypothesis Association," in *ACMMM*, 2020, pp. 3127–3135.

[20] C. Liu, Y. Jin, K. Xu, G. Gong, and Y. Mu, "Beyond Short-Term Snippet: Video Relation Detection with Spatio-Temporal Global Context," in *CVPR*, 2020, pp. 10 840–10 849.

[21] S. Ren, K. He, R. Girshick, and J. Sun, "Faster R-CNN: Towards Real-Time Object Detection With Region Proposal Networks," in *NeurIPS*, 2015, pp. 91–99.

[22] A. Bewley, Z. Ge, L. Ott, F. Ramos, and B. Upcroft, "Simple Online and Realtime Tracking," in *ICIP*. IEEE, 2016, pp. 3464–3468.

[23] N. Wojke, A. Bewley, and D. Paulus, "Simple Online and Realtime Tracking With a Deep Association Metric," in *ICIP*. IEEE, 2017, pp. 3645–3649.

[24] X. Shang, D. Di, J. Xiao, Y. Cao, X. Yang, and T.-S. Chua, "Annotating Objects and Relations in User-Generated Videos," in *ICMR*, 2019, pp. 279–287.

[25] J. Zhang, M. Elhoseiny, S. Cohen, W. Chang, and A. Elgammal, "Relationship Proposal Networks," in *CVPR*, 2017, pp. 5678–5686.

[26] J. Yang, J. Lu, S. Lee, D. Batra, and D. Parikh, "Graph R-CNN for Scene Graph Generation," in *ECCV*, 2018, pp. 670–685.

[27] Y.-W. Chao, Y. Liu, X. Liu, H. Zeng, and J. Deng, "Learning to Detect Human-Object Interactions," in *WACV*. IEEE, 2018, pp. 381–389.

[28] G. Gkioxari, R. Girshick, P. Dollár, and K. He, "Detecting and Recognizing Human-Object Interactions," in *CVPR*, 2018, pp. 8359–8367.

[29] Y.-L. Li, S. Zhou, X. Huang, L. Xu, Z. Ma, H.-S. Fang, Y. Wang, and C. Lu, "Transferable Interactiveness Knowledge for Human-Object Interaction Detection," in *CVPR*, 2019, pp. 3585–3594.

[30] D. Xu, Y. Zhu, C. B. Choy, and L. Fei-Fei, "Scene Graph Generation by Iterative Message Passing," in *CVPR*, 2017, pp. 5410–5419.

[31] R. Zellers, M. Yatskar, S. Thomson, and Y. Choi, "Neural Motifs: Scene Graph Parsing With Global Context," in *CVPR*, 2018, pp. 5831–5840.

[32] K. Tang, H. Zhang, B. Wu, W. Luo, and W. Liu, "Learning to Compose Dynamic Tree Structures for Visual Contexts," in *CVPR*, 2019, pp. 6619–6628.

[33] K. Tang, Y. Niu, J. Huang, J. Shi, and H. Zhang, "Unbiased Scene Graph Generation From Biased Training," in *CVPR*, 2020, pp. 3716–3725.

[34] S. Woo, J. Noh, and K. Kim, "Tackling the Challenges in Scene Graph Generation with Local-to-Global Interactions," *arXiv preprint arXiv:2106.08543*, 2021.

[35] K. He, G. Gkioxari, P. Dollár, and R. Girshick, "Mask R-CNN," in *CVPR*, 2017, pp. 2961–2969.

[36] K. He, X. Zhang, S. Ren, and J. Sun, "Deep Residual Learning for Image Recognition," in *CVPR*, 2016, pp. 770–778.

[37] T.-Y. Lin, M. Maire, S. Belongie, J. Hays, P. Perona, D. Ramanan, P. Dollár, and C. L. Zitnick, "Microsoft coco: Common objects in context," in *ECCV*. Springer, 2014, pp. 740–755.

[38] O. Russakovsky, J. Deng, H. Su, J. Krause, S. Satheesh, S. Ma, Z. Huang, A. Karpathy, A. Khosla, M. Bernstein *et al.*, "Imagenet large scale visual recognition challenge," *IJCV*, vol. 115, no. 3, pp. 211–252, 2015.

[39] B. Thomee, D. A. Shamma, G. Friedland, B. Elizalde, K. Ni, D. Poland, D. Borth, and L.-J. Li, "YFCC100M: The New Data in Multimedia Research," *Communications of the ACM*, vol. 59, no. 2, pp. 64–73, 2016.

[40] T. N. Kipf and M. Welling, "Semi-Supervised Classification With Graph Convolutional Networks," *ICLR*, 2017.



Sangmin Woo is currently working toward the M.S. degree in Electrical Engineering and Computer Science at Gwangju Institute of Science and Technology (GIST), Gwangju, Korea. He received a B.S. degree in Electrical Engineering from Kyungpook National University, Daegu, Korea, in 2019. His research interests include computer vision, visual understanding, and deep learning. He is a student member of the IEEE.



Junhyung Noh is a postdoctoral researcher at Lawrence Livermore National Laboratory (LLNL). He received the B.S. in Computer Science and Engineering & Statistics from Seoul National University in 2013, and the M.S. and Ph.D. in Computer Science Engineering from Seoul National University in 2015 and 2020, respectively. His research has focused on artificial intelligence, machine learning, and computer vision with a particular interest in object detection and its related high-level vision tasks such as semantic/instance segmentation, scene understanding, and image captioning.



Kangil Kim received the B.S. degree in computer science from the Korea Advanced Institute of Science and Technology, Daejeon, South Korea, in 2006, and the Ph.D. degree from Seoul National University, Seoul, South Korea, in 2012. He was a Senior Researcher with the Natural Language Processing Group, Electronics and Telecommunications Research Institute, Seoul, until 2016, and an Assistant Professor with the Computer Science and Engineering Department, Konkuk University, until 2019. He is currently an Assistant Professor with the Electronics Engineering and Computer Science Department and Artificial Intelligence Graduate School, Gwangju Institute of Science and Technology, Gwangju, South Korea. His research interests include artificial intelligence, evolutionary computation, machine learning, and natural language processing.